Science of the Total Environment 959 (2025) 178253

Contents lists available at ScienceDirect

Science of the Total Environment

journal homepage: www.elsevier.com/locate/scitotenv

Phytoplankton assemblages in the Southwestern Atlantic reef waters using HPLC-CHEMTAX approach

Antonia Diana Alves Bezerra [a,*], Hortência de Sousa Barroso [a], Carlos Rafael Borges Mendes [b], Luiz C. Cotovicz Jr. [c,d], Tallita Cruz Lopes Tavares [a], Tatiane Martins Garcia [a], Michael Barbosa Viana [a], Marcelo Oliveira Soares [a]

[a] Instituto de Ciências do Mar (LABOMAR), Universidade Federal do Ceará, Av. da Abolição, 3207, Meireles, 60165-081 Fortaleza, CE, Brazil
[b] Instituto de Oceanografia, Universidade Federal do Rio Grande (FURG), Av. Itália, km 8, Rio Grande, RS 96203-900, Brazil
[c] Department of Marine Chemistry, Leibniz Institute for Baltic Sea Research, Warnemünde, Germany
[d] Centro de Estudos do Mar, Universidade Federal do Paraná, Pontal do Paraná, PR, 83255-976, Brazil

HIGHLIGHTS

- Horizontal environmental homogeneity masked phytoplankton dynamics.
- The reefs did not significantly increase phytoplankton biomass.
- Benthic–pelagic coupling drove nutrient dynamics.
- Reefs caused shifts in phytoplankton community structure.

GRAPHICAL ABSTRACT

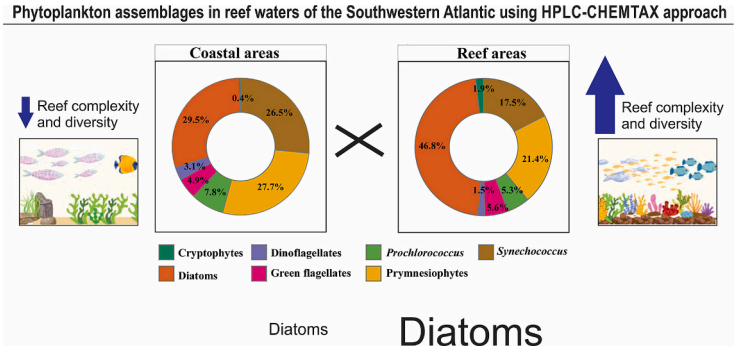

ARTICLE INFO

Editor: Olga Pantos

Keywords:
Coral reefs
Phytoplankton biomass
Diatoms
Dissolved inorganic nutrients
High-performance liquid chromatography

ABSTRACT

Understanding phytoplankton assemblages in reef waters is vital to comprehend their spatial variation and overall productivity. However, global research on these assemblages remains limited, especially using pigment-based high-performance liquid chromatography (HPLC)-CHEMTAX approach. Therefore, in this study, we compare the phytoplankton assemblages in the Southwestern Atlantic, including reef areas and coastal reefless areas, using the HPLC-CHEMTAX method. Water column analysis revealed well-oxygenated conditions, with euphotic zones extending from 8.6 up to 15.1 m. Similarities in abiotic variables between surface and mid-water samples indicated a thoroughly mixed water column. Phosphate and dissolved inorganic nitrogen (DIN) concentrations remained low, ranging from ≤0.14 to 0.64 and ≤ 0.10 to 1.51 μM, respectively. Dissolved reactive silicon (DSi) concentrations varied from ≤0.14 to 23.12 μM, with high concentrations observed in coastal samples. Overall, phytoplankton biomass was modest, with total chlorophyll *a* levels ranging from 0.18 to 0.91 mg m^{-3}. Diatoms, prymnesiophytes, and picocyanobacteria accounted for 91.2 % of the total biomass, whereas green flagellates, dinoflagellates, and cryptophytes made minor contributions. Phytoplankton composition differed between reefs and coastal areas, but no significant differences were found in the total biomass. Diatoms

* Corresponding author.
E-mail address: diannabezerra13@yahoo.com.br (A.D.A. Bezerra).

https://doi.org/10.1016/j.scitotenv.2024.178253
Received 18 June 2024; Received in revised form 12 December 2024; Accepted 20 December 2024
Available online 28 December 2024
0048-9697/© 2024 Elsevier B.V. All rights are reserved, including those for text and data mining, AI training, and similar technologies.

were prevalent, especially near the reefs, where a decrease in silica concentrations was observed. In contrast, *Synechococcus* and prymnesiophytes contributed more nearshore and beyond the reef areas. The distinct phytoplankton composition near reefs, even in oligotrophic waters, underscores the important role of tropical reefs in shaping phytoplankton assemblages via benthic–pelagic coupling.

1. Introduction

Phytoplankton contributes to approximately half (46.2 %) of the global primary productivity (Field et al., 1998). Moreover, productivity in continental shelves is approximately 3–5 times greater than that in the open sea, although sea shelf only accounts for approximately 7 % of the ocean surface area (Simpson and Sharples, 2012). Continental shelves provide 90 % of the global fisheries (Pauly et al., 2002), and phytoplankton primary production is fundamental to this supply (Pauly and Christensen, 1995; Stock et al., 2017).

Tropical coasts are characterized by interconnected reef systems (Roelfsema et al., 2013). Along the Equatorial Southwestern Atlantic Ocean, covering approximately 1000 km in the SE-NW direction, lies the Brazilian semiarid coast (SAC) (from 5° S 36° W to 2° S 44° W). SAC is located halfway between the Amazon Reef System (ARS) and Eastern Brazilian Reef System (ERS) (Carneiro et al., 2022; Costa et al., 2024). The hard-bottom formations covered by biogenic carbonate sediments along the SAC (Knoppers et al., 1999a) connect the ARS and ERS, forming a unique ecosystem considered as one of the largest semi-continuous tropical marine ecosystems in the world (Carneiro et al., 2022).

These complex reef systems, including that on the SAC, are characterized by various types of consolidated substrates that are often associated with other interconnected habitats, such as rhodoliths and seagrass beds (Carneiro and Morais, 2016; Carneiro et al., 2021). Moreover, the continental shelf in the SAC exhibits distinct environmental features, including significant interannual variability in precipitation, low river input, and strong influence of wind on the coastal landscape (Soares et al., 2021). Additionally, this low-latitude coast experiences consistently high temperatures (> 26 °C) throughout the year with minimal intra-annual variability (approximately 5 °C) (Teixeira and Machado, 2013; Soares et al., 2019a).

Only a few ecological studies have been conducted on the phytoplankton assemblages of the SAC continental shelf, mainly using traditional microscopy (e.g., Klein, 1977; Passavante et al., 1982; Moreira Filho et al., 1999; Franco et al., 2018) and flow cytometry (Saes, 2018). Although Utermöhl method using an inverted microscopy provides reliable numerical data on nano- and microphytoplankton, it underestimates picophytoplankton organisms (Edler and Elbrächter, 2010; Brito et al., 2015; Mendes et al., 2017). Inverted microscopy combined with epifluorescence or flow cytometry can be an alternative to account for all fractions (Crosbie and Furnas, 2001; Jacquet et al., 2006; Ke et al., 2016). However, high-performance liquid chromatography (HPLC) makes it possible to obtain data for all fractions (Schlüter et al., 2011) through a single high-precision technique that allows automated and rapid analysis of a large number of samples (Wright and Jeffrey, 2006).

Studies exploring the western Atlantic Ocean using flow cytometry (Menezes et al., 2023) and HPLC (Farias et al., 2022) revealed the marked contribution of pico- (Menezes et al., 2023; Farias et al., 2022) and nano-phytoplankton (Farias et al., 2022) to the structure of phytoplankton assemblages. Small phytoplankton organisms may be prevalent due to the nutrient-poor conditions in tropical oceans and coastal areas (Waterbury et al., 1979; Hillebrand et al., 2022). However, the influence of nutrients on cell size may also be intricately associated with other factors such as seawater temperature and grazing (Pomati et al., 2020; Hillebrand et al., 2022).

Previous studies comparing phytoplankton structure between coral reef waters and the adjacent ocean have shown that phytoplankton can undergo shifts in composition and biomass in waters overlying reefs (e.g., Furnas et al., 1990; Van Duyl et al., 2002). For example, due to complex interactions between bottom and overlying reef waters, a decrease in phytoplankton biomass can occur through selective grazing by reef suspension feeders (Ribes et al., 2005; Houlbrèque et al., 2006; Genin et al., 2009), which has the potential to influence phytoplankton composition (Hoadley et al., 2021). On the other hand, studies in oligotrophic waters have also reported an enhancement in phytoplankton biomass around reef formations (Jales et al., 2015; Vollbrecht et al., 2021).

Our study aimed to compare the biomass and composition of phytoplankton in the SAC (Equatorial Southwest Atlantic) between a protected reef area and the surrounding coastal reefless areas, testing the hypothesis that there are differences between these areas related to environmental gradients. This knowledge is crucial in shallow (<30 m) and well-mixed areas where benthic–pelagic coupling significantly affects the spatial dynamics of primary producers (Rossi and Gili, 2009). In addition, using the HPLC method, we will shed light on the composition of phytoplankton in the SAC. Although for oligotrophic tropical coastal regions it is common to expect the predominance of picocyanobacteria (Charpy et al., 2012; Farias et al., 2022), due to the gap in studies using methods that include the entire phytoplankton community in the SAC (e.g., HPLC-CHEMTAX), other groups may be revealed as contributing more to the biomass.

2. Material and methods

2.1. Study area

The study area was located in the Brazilian semiarid coast (SAC), with 10 sampling marine stations between 1.74 and 26.9 km away from the coast. Some stations (S3 to S7), encompass the marine protected area (MPA) known as “Pedra da Risca do Meio State Marine Park” (PEMPRIM) (Fig. 1). Despite sea surface temperatures exhibiting spatial and temporal homogeneity (Teixeira and Machado, 2013; Barroso et al., 2023), the area demonstrates spatial heterogeneity due to shifts in bathymetry, coastal current directions, and the presence of reef ecosystems, mainly inside the MPA (Fig. 1). In this MPA, the main carbonate reef builders are crustose coralline algae and four coral species, mainly the reef-building coral *Siderastrea stellata*. The local circulation at the stations near the coast and the MPA is similar and predominantly from east to west by coastal currents (Costa et al., 2024). This complexity is responsible for the diversity in this low-latitude continental shelf, which remains relatively understudied despite its ecological significance (Dias et al., 2013; Soares et al., 2017; Cotovicz et al., 2020).

This MPA has tropical reefs (geogenic and biogenic), with a significant cover of macroalgae, sponges, and reef-building corals with a low height in relation to the ocean floor (1 to 3 m). (Soares et al., 2017; Carneiro et al., 2022). The MPA ichthyofauna is composed of 131 taxa (in 54 families), and presents 63.3 % of the reef fish species recorded in Ceará (Freitas et al., 2019). Covering a rectangular expanse of 33.20 km^2, the MPA lies approximately 18 km from the city of Fortaleza, the capital of Ceará State (Brazil) (Fig. 1), with tropical reefs varying in depth from 16 to 30 m (Soares et al., 2011, 2017). Moreover, the coastal reefless areas (outside the MPA) have submerged dunes and a large quantity of carbonate and siliciclastic sediments (Soares et al., 2017; Carneiro et al., 2022) (Fig. 1).

2.2. Sampling

Oceanographic sampling was conducted in July 2019 at all 10 stations (Fig. 1), with one station (S1) situated near the coast, five stations (S3, S4, S5, S6 and S7) within the reef region protected by the MPA, and four stations (S2, S8, S9 and S10) around the MPA (Fig. 1). The minimum distances from the stations located within the reef region to the nearest reef cover ranged from 1.1 (S5) to 2.5 (S6) km, while the four surrounding stations had minimum distances of 4.6 (S2) to 9.6 km (S10) (Table S1). In terms of depth, the sampled area was relatively shallow, with values ranging from 16.5 to 28.8 m. Station S1 was the shallowest, while stations S6 (28.8 m) and S9 (27.7 m) were the deepest (Table S1). Please see Table S1 in the Supplementary material for more details.

Water samples for phytoplankton pigment analysis, and nutrient assessment were collected using Van Dorn bottles at both the surface (0.15 m below) and mid-water depths (8–14 m). The depth, vertical temperature, and salinity profiles were measured using a CTD CastAway model. Dissolved oxygen (DO) levels were recorded using a multiparametric probe (YSI Professional Plus model). Water transparency was estimated using the Secchi disk, and the euphotic zone depth (Z_{eu}) was calculated as 2.7 times the Secchi depth (Cole, 1983).

2.3. Nutrient and pigment analyses via HPLC

For the analysis of dissolved inorganic nutrients, the samples were immediately filtered onboard after collection. For nitrate ($N\text{-}NO_3^-$) plus nitrite ($N\text{-}NO_2^-$), N-ammoniacal (NNH_3+ $N\text{-}NH_4^+$), and phosphate ($P\text{-}PO_4^{3-}$), 1 L of water was filtered through glass fiber filters (0.7 μm pore size GF-3; Macherey-Nagel, Düren, Germany). Dissolved reactive silicon (DSi) was filtered through a mixed cellulose ester membrane (0.45 μm pore size, HATF; Millipore, Billerica, USA) in 300 ml aliquots. After filtration, all samples were stored at 4 °C in the dark until transported to the laboratory and then stored at −20 °C until analysis. $N\text{-}NO_3^-$, $N\text{-}NO_2^-$, $P\text{-}PO_4^{3-}$ and DSi were analyzed according to the protocol by Aminot and Chaussepied (1983) described in Baumgarten et al. (1996). For N-ammoniacal analysis, it followed the protocol of Strickland and Parsons (1972) described in Baumgarten et al. (1996). The concentrations of $N\text{-}NO_3^-$, $N\text{-}NO_2^-$ and N-ammoniacal were summed and presented as total dissolved inorganic nitrogen (DIN). All laboratory analyzes were performed in triplicate, with detection limits (DL) of 0.05 μM, 0.10 μM, 0.06 μM and 0.14 μM for $P\text{-}PO_4^{3-}$, $N\text{-}NO_3^-$ plus $N\text{-}NO_2^-$, N-ammoniacal and DSi, respectively.

For pigment analysis, volumes of seawater ranging from 0.10 to 1.0 l were filtered through Whatman GF/F glass microfiber filters (pore size 0.7 μm, 25 mm diameter) under vacuum pressure of <5 in. of Hg and in low light. After filtration, the samples were immediately stored in liquid nitrogen for rapid freezing of the cells and, later, they were stored at −80 °C until extraction. For pigment extraction, the filters were placed in centrifuge tubes with 3 ml of cold buffered 95 % methanol (2 % ammonium acetate), containing 0.05 $mg.ml^{-1}$ of trans-β-apo-8′-carotenal as an internal standard and subsequently macerated with a glass rod. The samples were stored for 30 min at −20 °C, then ultrasonicated for 5 min in a cold bath, and stored again for another 30 min at −20 °C. At the end of the extraction step, the samples were centrifuged in a refrigerated centrifuge at 2 °C for 5 min at 3500 rpm. The supernatant was then filtered using a 0.2 μm pore Millipore PTFE membrane filter. In

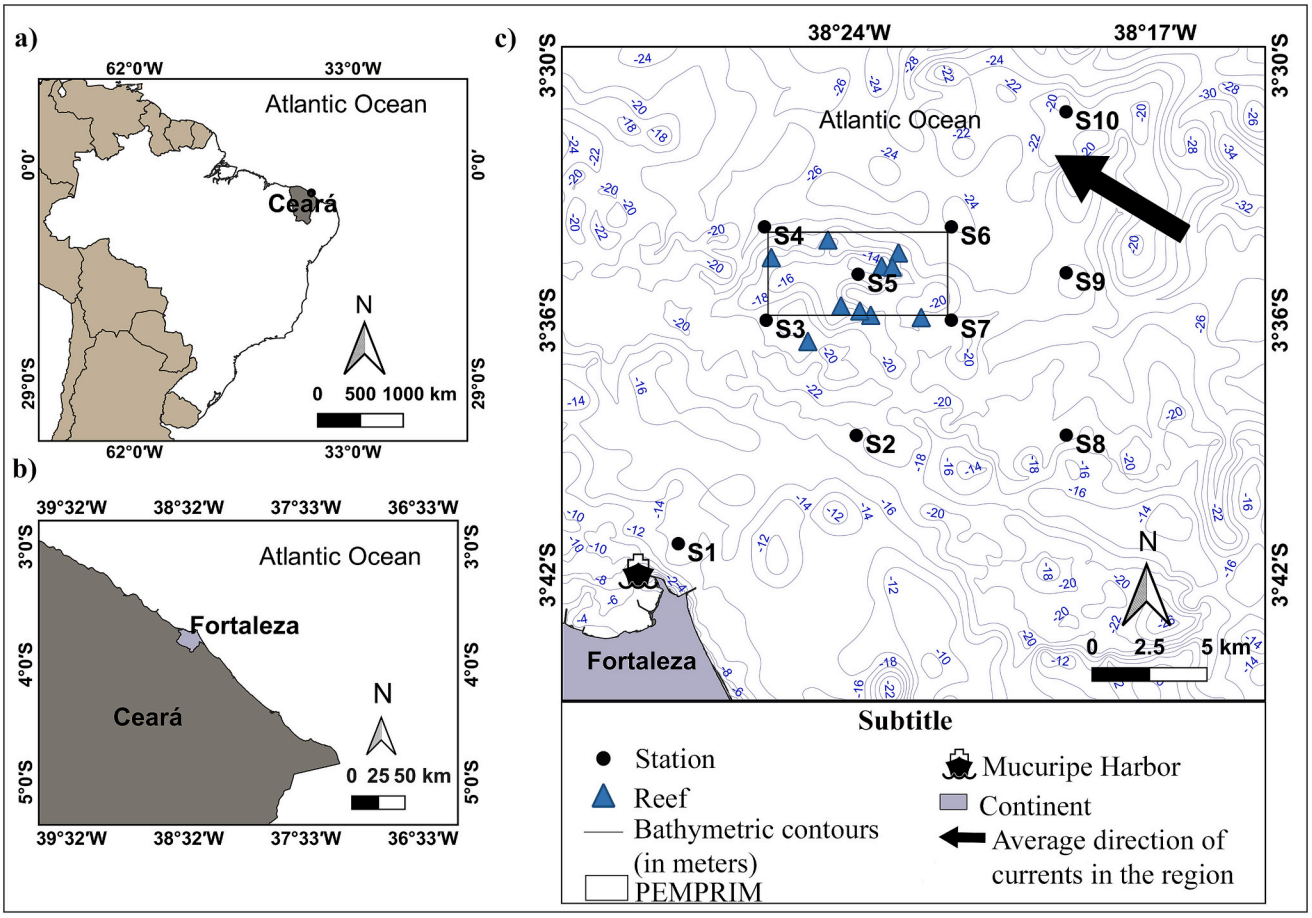

Fig. 1. Geographical location of the Marine Protected Area (MPA) - Pedra da Risca do Meio State Marine Park (PEMPRIM), on the continental shelf of the Equatorial Southwestern Atlantic, State of Ceará, Brazil (a). Location of the MPA off the coast of Fortaleza, Ceará (b). Sampling stations (S1–S10), bathymetric contours (in meters) and MPA indicated by the rectangular region (c).

specific vials for chromatography, an aliquot of 1000 μl of sample was mixed with 400 μl of Milli-Q water and the solution was injected into the Shimadzu HPLC with refrigeration at 4 °C.

The HPLC used is equipped with a degasser (DGU-20 A), a solvent distributor module (LC-20 CE), an automatic sample injector (SIL-20 AC), a photodiode array detector (SPD-M20A; wavelength 190 to 800 nm, 1 nm spectral resolution), a column oven (CTO-20 AC), and a fluorescence detector (RF-10AXL; excitation 430 nm/emission 670 nm). The method adopted for the identification of chlorophylls and carotenoids by HPLC is described in Zapata et al. (2000), using a reversed-phase C8 monomeric column with a mobile phase containing pyridine. The limits of detection and quantification of the referred method are duly described/discussed in Mendes et al. (2007).

From their absorbance spectra and retention times, the pigments present in the samples were identified and quantified. Their concentrations were calculated from the signals obtained by the photodiode detector in comparison with commercial standards of pigments obtained at DHI (Institute of Water and Environment, Denmark), which were used for HPLC calibration. For peak integration, the LCSolution program (Shimadzu) was used, and all integrations were manually verified and corrected whenever necessary.

2.4. CHEMTAX analysis of pigment data

After determining the concentrations of specific marker pigments for the phytoplankton groups and chlorophyll *a* levels, their relative contributions to the total chlorophyll *a* (Tchl *a* = Chl *a* + DVChl *a*) levels were quantified using the CHEMTAX chemical taxonomy program developed by Mackey et al. (1996) and optimized by Wright et al. (2009). CHEMTAX analysis is described in detail in the Supplementary material.

The initial pigment ratios of major algal groups used here were compiled from Higgins et al. (2011) (see Table S2), preferably using, when available, the ratios obtained from field data. Based on the identified diagnostic pigments, eight algal groups were loaded into the CHEMTAX software, namely green flagellates (including those with chlorophyll *b*: chlorophytes and prasinophytes), dinoflagellates, cryptophytes, prymnesiophytes, *Synechococcus*, *Prochlorococcus*, and diatoms. Additionally, two types of diatoms were defined: Type 1, containing typical diatom pigmentation (chlorophylls c_1, c_2, fucoxanthin, diadinoxanthin), and Type 2, where chlorophyll c_3 replaces chlorophyll c_1 – typified by *Pseudonitzschia* sp. (Zapata et al., 2011), which were commonly observed in our samples. These chemotaxonomic groups were identified as described by Jeffrey et al. (2011) (see Table S3).

2.5. Statistical analyses

For all statistical analyses, we considered the samples from surface and mid-water separately; that is, we used 10 samples for reef stations (S3, S4, S5, S6, and S7: surface and mid-water) and 10 for surrounding coastal waters (S1, S2, S8, S9, and S10: surface and mid-water).

We assessed the normality of total biomass (refers to Tchl *a*) using the Shapiro-Wilk test (Souto and Souto, 2020). Since the data showed a non-normal distribution, we used the Wilcoxon test (Mann–Whitney) to examine the significant differences between samples from reefs and coastal areas ($p < 0.05$) (Souto and Souto, 2020). The normality of the biomass of each phytoplankton group was also analyzed and only diatoms type 2 followed a normal distribution. These statistical analyses were carried out using the PAST v.4.02 program (Hammer et al., 2001).

Differences in phytoplankton assemblages between the protected reef area (i.e., MPA) and the surrounding coastal waters were assessed using non-metric multidimensional scaling (NMDS) based on Bray–Curtis distance, followed by an analysis of similarities (ANOSIM) using 999 permutations. For NMDS and ANOSIM we used the non-transformed absolute biomass of phytoplankton groups, as both analyses are non-parametric and do not require normality (Xia, 2020; Bakker, 2024). To reveal the environmental gradient and explore the relationship between environmental variables (temperature, salinity, P-PO_4^{3-}, DSi, and DIN) and phytoplankton assemblages structure, we employed the "envfit" method (Borcard et al., 2018). Since environmental variables were measured in different scales, before the "envfit" they were transformed by log (x + 1). All these analyses were performed using the R package "vegan" (version 2.6–8) (functions "metaMDS", "anosim" and "envfit" using 999 permutations) (Oksanen et al., 2024) in R 4.3.1. NMDS plot was visualized using R package "ggplot2" (version 2.6–8) (Wickham, 2016).

To visualize the spatial distribution of total biomass, absolute biomass of phytoplankton groups and abiotic variables (nutrients, temperature, and salinity), we used Ocean Data View v.4.7.8 (Schlitzer, 2016) with a weighted average grid function (scale length 70 for X and Y) to interpolate the data.

3. Results

3.1. Environmental variables

The surface layer exhibited high dissolved oxygen saturation (101 ± 1.2 %) (Table S1). The depth of the euphotic zone ranged from 8.6 to 15.1 m, with the maximum limits often closely associated with mid-water depths (Table S1). Water transparency varied, with minimum and maximum values of 3.2 and 5.6 m recorded at S10 (station farthest from the coast) and S2 (coastal surroundings), respectively (Table S1). Temperature (Fig. 2a and b) and salinity (Fig. 2c and d) showed minimal spatial and vertical variations (Table S1; Fig. S1) with mean values of 27.8 °C ± 0.06 and 36.2 ± 0.14, respectively (Table S1).

$P^{-}PO_4^{3-}$ concentrations ranged from ≤0.05 to 0.64 μM across the area, indicating consistently low levels (Fig. 2e and f). Similarly, DIN concentrations ranged from ≤0.06 to 1.51 μM, with most samples having concentrations <1.0 μM, except for mid-water samples from S6 (1.51 μM) (inside reef) and S8 (1.13 μM), and S10 (1.01 μM) in coastal surroundings (Fig. 2g and h).

Regarding DSi concentrations (≤ 0.14 to 23.1 μM), most of the samples showed low concentrations (<1 μM), especially on the reefs. However, high concentrations were observed at some stations in the surrounding coastal zone, namely at S1 (the closest to the coast) (surface: 23.1; mid-water: 14.1 μM), S2 (in mid-water: 7.3 μM) and S10 (in mid-water: 5.6 μM) (Fig. 2i and j).

In all samples except for S1, the DSi:DIN ratios were <6. At S1, the ratios were 27.9 at the surface and 37.6 at mid-water (Table S5). In turn, the DSi:PO_4^{3-} ratios were generally lower than 3, except for some stations located in the surrounding coastal zone, these being the samples from S1 (> 30) and the mid-water samples from S2 and S10 (> 22) (Table S5). For DIN:PO_4^{3-} ratios remained consistently low (always <5) in both the reef area and their surroundings. Please see Table S4 in the Supplementary material for more details.

3.2. Pigment concentrations, biomass, and composition of phytoplankton assemblages

A total of 21 phytoplankton pigments were identified by HPLC analysis (Table S5). Chlorophyll *a* (average Chl *a* = 0.34 ± 0.14 mg m^{-3}), zeaxanthin (average Zea = 0.12 ± 0.05 mg m^{-3}), and fucoxanthin (average Fuco = 0.10 ± 0.05 mg m^{-3}) were the pigments with the highest concentrations and were present in all the samples. The lowest concentration of Chl *a* (present in all groups except *Prochlorococcus*) was at the surface of the station closest to the coast (S1 = 0.17 mg m^{-3}), while the highest concentration was observed in the mid-water of S9 (surroundings east of the reefs, Chl *a* = 0.84 mg m^{-3}). In the reef areas, the highest concentrations of Chl *a* were in the mid-water of stations S5 (0.52 mg m^{-3}) and S7 (0.44 mg m^{-3}). The pigment Zea (dominant in *Synechococcus* and present in *Prochlorococcus*) showed higher

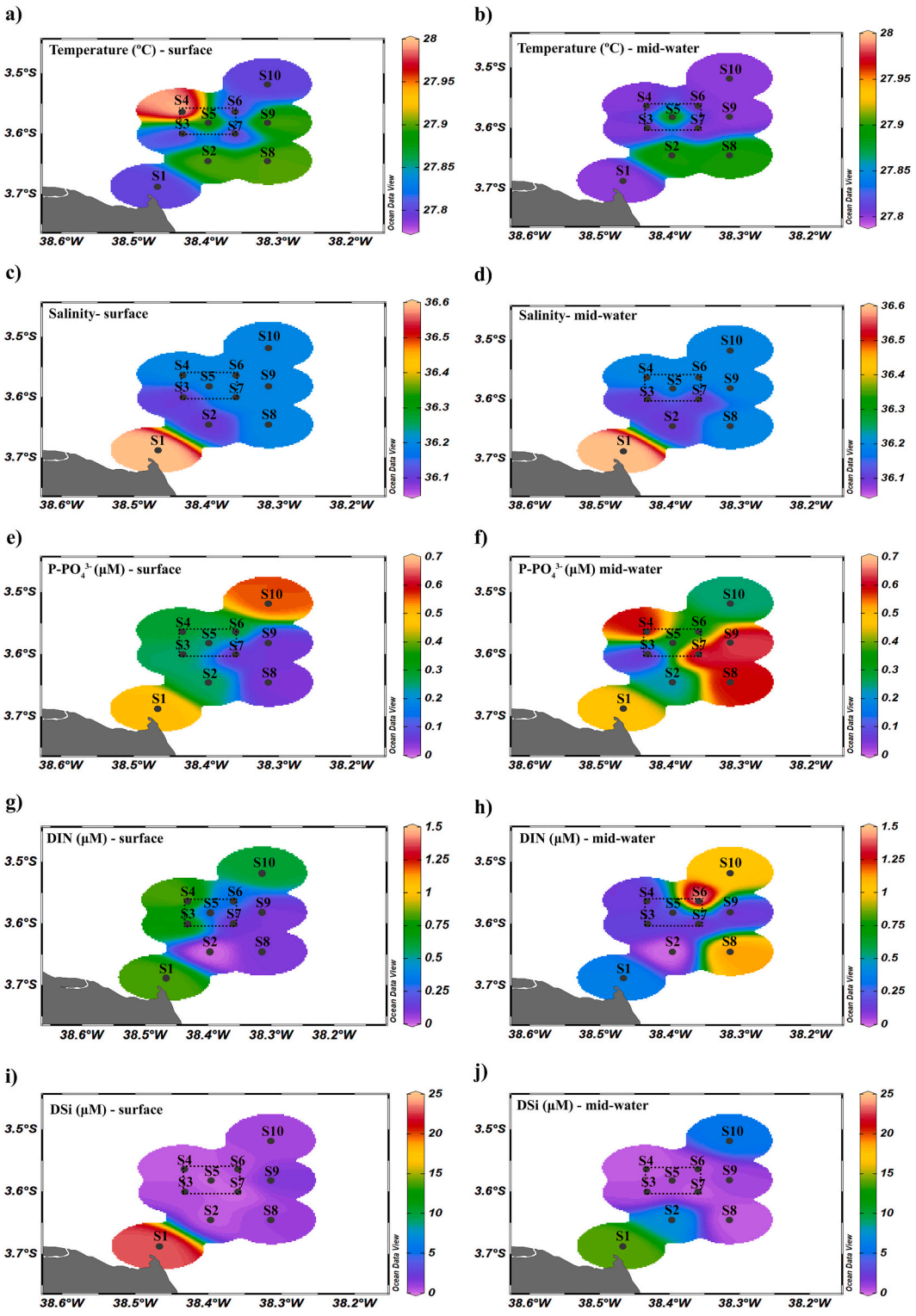

Fig. 2. Distribution of temperature (°C), salinity and nutrient concentrations (µM) in surface and mid-water samples of the semi-arid continental shelf of the Equatorial Southwestern Atlantic (Ceará, Brazil). (a and b) – temperature; (c and d) – salinity; (e and f) – phosphate ($P\text{-}PO_4^{3-}$); (g and h) – dissolved inorganic nitrogen (DIN); (i and j) – dissolved reactive silicon (DSi). The main reef area (MPA) is indicated by the black dotted rectangle (S3, S4, S5, S6, and S7). Note the different color scales.

concentrations in the surrounding coastal zone (mid-water of S1 = 0.22 mg m^{-3} and S9 = 0.26 mg m^{-3}). In turn, in the reef area, Zea ranged from 0.08 to 0.11 mg m^{-3}. Fuco pigment (dominant in diatoms and present in prymnesiophytes) was higher in the mid-water of S9 (surrounding coastal; 0.24 mg m^{-3}) and S5 (reef area; Fuco = 0.19 mg m^{-3}).

Tchl *a* (phytoplankton biomass index) concentrations ranged from 0.18 mg m^{-3} (surface) at the station close to the coast (S1) to 0.91 mg m^{-3} (S9 mid-water) east of the reefs (Fig. 3a and b). Except for S9, located in the coastal zone, the highest Tchl *a* levels were observed in the reef zone (S5, S6, S7). Despite the increase in some stations from the reef

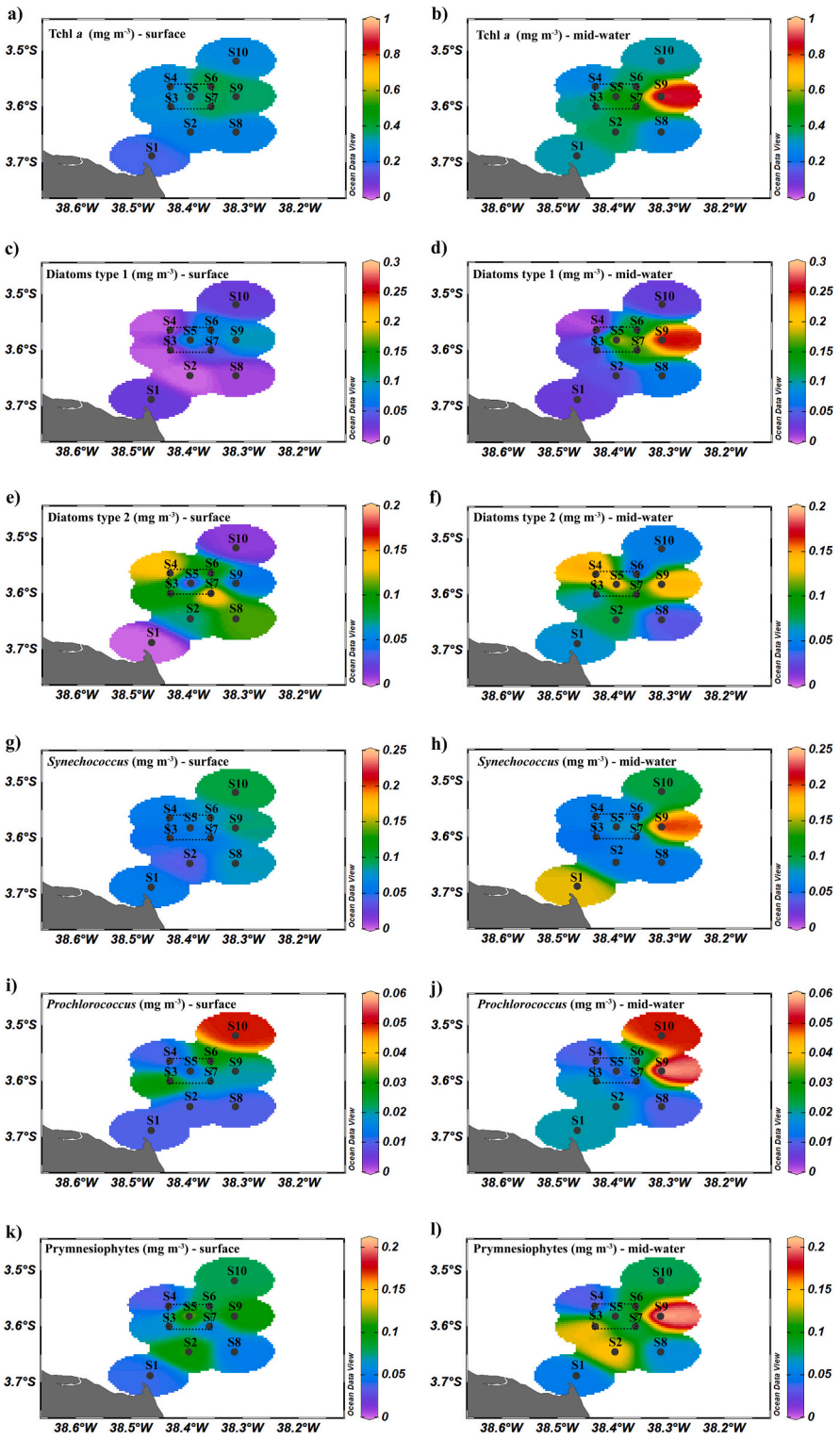

Fig. 3. Distribution of total chlorophyll *a* concentration (Tchl *a*) and absolute contribution of the main groups for Tchl *a* (mg m^{-3}) in surface and mid-water samples on the semiarid continental shelf of the Equatorial Southwestern Atlantic (Ceará, Brazil): (a and b) – Tchl *a*; (c and d) – diatoms type 1; (e and f) – diatoms type 2; (g and h) – *Synechococcus*; (i and j) – *Prochlorococcus*, and (k and l) – prymnesiophytes. The main reef area (MPA) is indicated by the black dotted rectangle (S3, S4, S5, S6 and S7). Note the different color scales.

area, the averages were similar in both areas (reefs: 0.36 ± 0.08 mg m^{-3}; surrounding areas: 0.36 ± 0.19 mg m^{-3}) and no significant differences were observed.

Analyzing the phytoplankton assemblages according to the presence of reefs, an increase in diatoms was observed in this area, comprising nearly 50 % of the total relative contribution (Figs. 4b, 3c–f, and Table S6). In contrast, coastal areas showed a more equitable distribution, with diatoms, *Synechococcus*, and prymnesiophytes each presenting similar contributions of around 30 % (Figs. 4a and 3g–j).

Across the entire area, diatoms (type 1 and type 2) were also the most relevant group, comprising 38.2 % of the total composition, followed by picocyanobacteria (*Synechococcus* and *Prochlorococcus*; 28.5 %; Fig. 4c

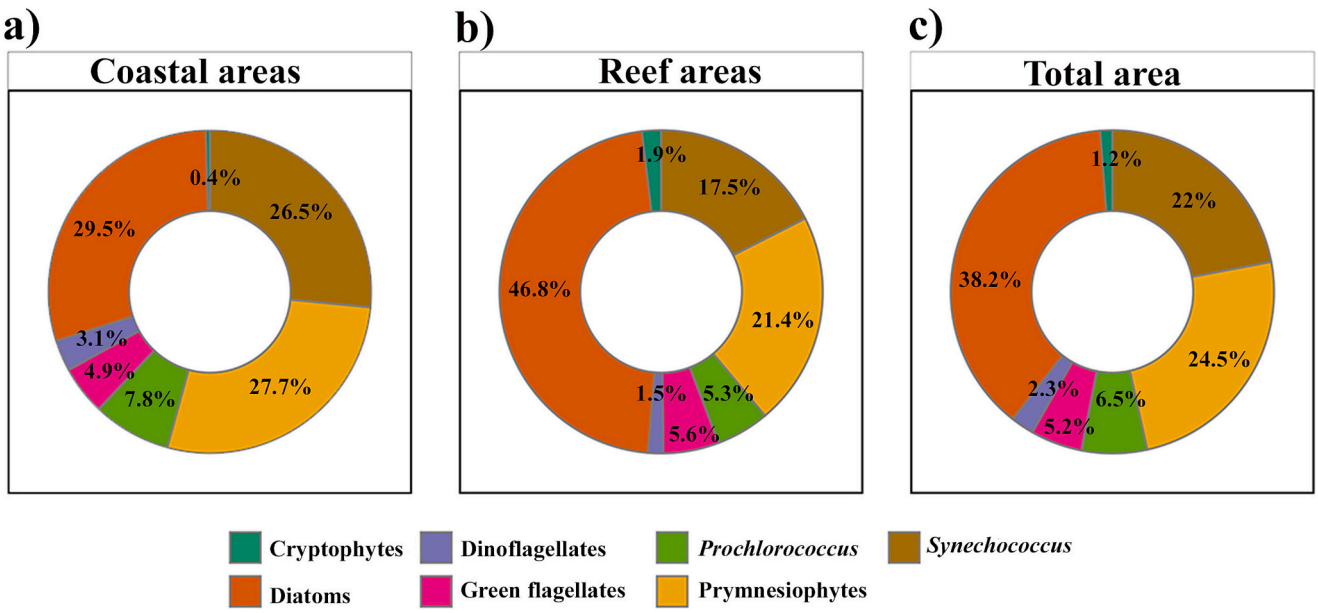

Fig. 4. Average relative contribution of phytoplankton groups in the study area (semi-arid continental shelf of the Equatorial Southwestern Atlantic, Ceará, Brazil) considering the a) surrounding coastal reefless areas, b) reef area, and c) total area.

and Table S6) and prymnesiophytes (24.5 %; Figs. 4c and 3k and l). Green flagellates, dinoflagellates, and cryptophytes exhibited low mean contributions (Fig. S2), accounting for 5.2, 2.3, and 1.2 % of the total biomass, respectively (Fig. 4c; Table S6). It is also important to highlight the spatial distribution of picocyanobacteria (Fig. 3g–j). While *Prochlorococcus* increased in the more distant stations (S9 and S10), *Synechococcus* was higher in the station close to the coast (S1), although it also increased in S9 (mid-water).

3.3. Structure of phytoplankton assemblages and relationship between abiotic variables and phytoplankton

In order to understand the effects of reefs on the general structure of phytoplankton assemblages, NMDS based on Bray–Curtis distance and ANOSIM were performed. In the NMDS plot, the phytoplankton assemblages were clustered according to the areas (Fig. 5). ANOSIM values across areas indicated a significant separation between phytoplankton assemblages from reefs and coastal surrounding areas ($R = 0.12$; $p <$

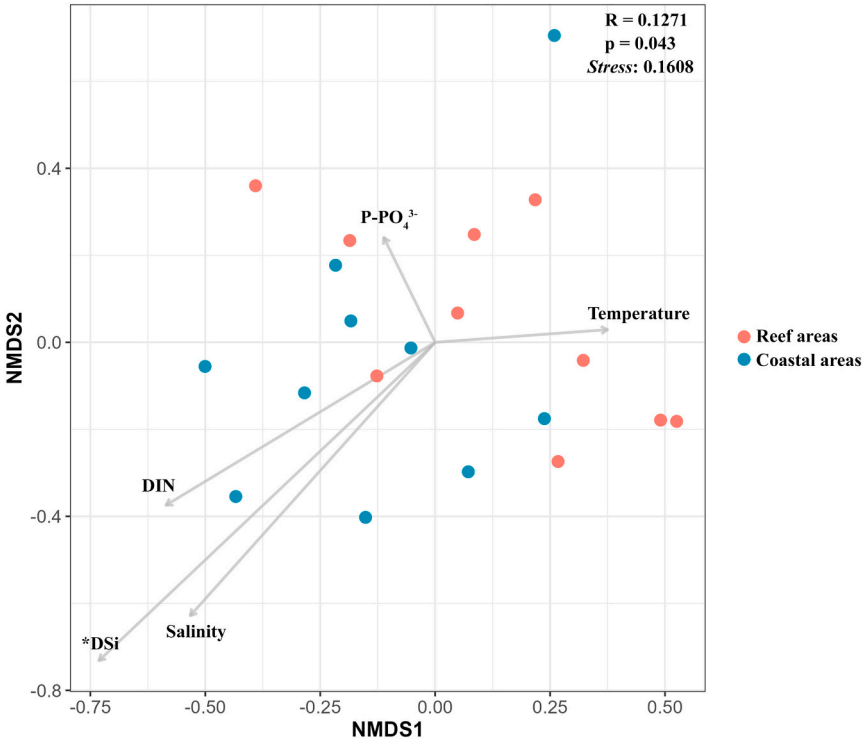

Fig. 5. Non-metric multidimensional scaling (NMDS) plot based on Bray–Curtis distance of the structure of phytoplankton assemblages with environmental parameters added using envfit. *DSi was the only statistically significant variable measured through the envfit test ($p < 0.05$). R and p values were calculated by an analysis of similarities (ANOSIM). DIN: Dissolved Inorganic Nitrogen. DSi: dissolved reactive silicon.

0.04). To reveal the environmental gradient and the relationship between the abiotic variables and phytoplankton assemblages structure, the "envfit" method was performed (Fig. 5). DSi was the only statistically significant variable ($r^2 = 0.3698$; $p = 0.016$), showing a negative correlation with both NMDS axes (Supplementary Table S7). In the NMDS plot, it is possible to see a negative association between DSi and the phytoplankton assemblages from reefs, indicating a higher consumption and demand for silicon in this area, which is consistent with the higher relative contribution of diatoms (Fig. 4).

4. Discussion

In this study, we observed a shift in the phytoplankton composition between stations in reef and coastal reefless areas via phytoplankton pigment fingerprinting using the HPLC-CHEMTAX approach. The results indicated oligotrophic conditions across the entire region and no significant difference was observed in the total phytoplankton biomass between reef areas and surrounding coastal areas. Nonetheless, it was possible to observe an increase in relative contribution of diatoms (phytoplankton assemblages) in the reef area (MPA). The local circulation at the stations near the coast and the MPA is similar and predominantly from east to west by coastal currents. Therefore, if the differences in the diatom communities were due to coastal circulation, they should be homogeneous throughout the area, but our results clearly show heterogeneity due to the presence of reefs. Indeed, despite the spatial homogeneity of the salinity and temperature data, heterogeneity was found for the nutrients, notably DSi. Thus, the lowest DSi contents in reefs was associated with higher diatom contributions likely due to consumption. Besides diatoms, other important groups in SAC were picocyanobacteria and prymnesiophytes.

4.1. Oligotrophy on the semiarid coast

The temperature and salinity data pointed to a horizontally homogeneous area. In turn, vertical temperature and salinity profiles indicated the absence of stratification, suggesting a well-mixed water column. Local hydrodynamic conditions, such as the semi-diurnal tidal regime, strong trade winds, and intense ocean currents, contribute to the high energy levels in the Southwestern Equatorial Atlantic shelf (Vital et al., 2008; Dias et al., 2013), maintaining water column homogeneity (Barroso et al., 2023).

Concentrations of dissolved inorganic nutrients fell within the range of previous surveys in the Tropical Southwestern Atlantic (DIN = 0.05–3.20 μM; P-PO_4^{3-} = 0.001–0.92 μM; DSi 0.07–70.0 μM) (Carvalho et al., 2017; Araujo et al., 2019). A commonly applied approach to understand the nutrient limitation in coastal and oceanic waters involves comparing in situ nutrient ratios with established thresholds that define the nutrient levels required for phytoplankton uptake, such as the classical Redfield and Brzezinski ratios (Redfield et al., 1963; Brzezinski, 1985). According to these researchers, for instance, diatoms require an Si:N:P molar ratio of 16:16:1, respectively. Another approach to infer nutrient limitation in coastal waters (Domingues et al., 2023) is to combine nutrient ratios and absolute concentrations, according to the following criteria: N limitation if DIN < 1 μM, N:P < 10, and DSi:N > 1; P limitation if PO_4^{3-} < 0.1 μM, N:P > 22, and DSi:P > 22; and Si limitation if DSi < 2 μM, Si:N < 1, and Si:P < 10 (Justić et al., 1995).

In the SAC region, in all samples the DIN:PO_4^{3-} ratio (< 5) was lower than the Redfield and Brzezinski molar ratio (16), indicating strong nitrogen limitation, which is also consistent with previous reports in the Southwest Tropical Atlantic (Araujo et al., 2019; Farias et al., 2022).

On the other hand, DSi:DIN ratios varied across the study area, and some differences between reef and coastal areas can be noted. In reefs (S3 and S4: surface; and S6: mid-water), low DSi:DIN ratios (<1) suggested DSi limitation and increased consumption by phytoplankton. Notably, at other depths of these stations (S3 and S4: mid-water; S6: surface), DSi:DIN molar ratios >1 suggested no DSi limitation. However, by the criterion of absolute DSi concentrations (Justić et al., 1995), which was <2 μM in all these samples, the potential Si limitation was corroborated in reefs. The highest relative contributions of diatoms in these samples (27–58.2 %), associated with an significant inverse correlation between this group and DSi concentrations corroborated the demand for this nutrient in tropical reefs.

For coastal areas, we highlight the station closer to the coast (S1), where high DSi:DIN ratios were observed, indicating high DSi availability and N limitation. At this station, *Synechococcus* was the group that contributed most to Tchl *a* (> 30 %), while diatoms contributed only around 15 %. Possibly, the high availability of DSi is due to continental input. In fact, the main source of DSi in seawater is continental input, mainly from rivers and groundwater (Tréguer and De La Rocha, 2013).

In relation to the DSi:PO_4^{3-} ratios <3, it was observed that in most samples, they were below the Redfield and Brzezinski molar ratio of 16, suggesting greater removal of DSi than of PO_4^{3-}. This reinforces DSi limitation especially in the reef area. DSi is an essential nutrient for siliceous primary producers (e.g., diatoms) and can become a limiting nutrient in oligotrophic waters (Sospedra et al., 2018).

Therefore, our data suggest a high demand for nitrogen and silica in the studied semiarid coast. However, these results should be interpreted with caution, as there is growing evidence that nutrient limitation in phytoplankton does not always adhere to the single nutrient limitation model (e.g., Domingues et al., 2023). Instead, co-limitation by multiple nutrients may be more likely in aquatic ecosystems (Elser et al., 2007). To test this hypothesis, alternative approaches are needed, such as investigating nutrient uptake kinetics and conducting experimental bioassays with factorial additions of nitrogen, phosphorus, and silica (Domingues et al., 2023; Ren et al., 2009).

Similar to inorganic nutrients, Tchl *a* levels were within a range previously reported in the continental shelf of the Brazilian northeast region (0.01–0.63 mg m^{-3}) (Carvalho et al., 2017), except for an unexplained concentration peak in the mid-water sample of station S9. The chlorophyll *a* values from satellite data for MPA exhibited small inter- and intra-annual variability with an average value of approximately 0.3 μg L^{-1}. The monthly climatological standard deviations for chlorophyll *a* were also small, usually <0.1 μg L^{-1}. Based on the remote sensing data, Barroso et al. (2023) also detected a small spatial variability within the area, with values ranging from 0.2 to 0.6 μg L^{-1} towards deeper regions.

Additionally, Tchl *a* concentrations were similar to find in other coral reef zones, for example, the fringing coral reefs of Sesoko Island, Japan (0.11–0.77 mg m^{-3}; annual mean = 0.45 mg m^{-3}) (Tada et al., 2003), Abrolhos Bank (0.17 ± 0.01–0.50 ± 0.09 mg m^{-3}) (Bruce et al., 2012), and Rocas Atoll (average = 0.10–0.91 mg m^{-3}) (Jales et al., 2021); being the last two are also part of the South Atlantic reef ecosystems.

Chlorophyll *a* concentration, as a proxy for phytoplankton biomass, is widely used in studies on the impact of eutrophication on coral reef health, because this variable responds quickly to the input of nutrients into the water column (Bell et al., 1989, 2014; Guo et al., 2019). Phytoplankton blooms can cause various stresses, compromising the survival of coral reefs by limiting the absolute concentration of nutrients, changes in the N:P ratio, light limitation, suffocation by mucus, production of toxins and depletion of dissolved oxygen (Guzmán et al., 1990). However, moderate levels of phytoplankton biomass may represent solar protection against light stress (D'Angelo and Wiedenmann, 2014; Keighan et al., 2023) and food availability for corals, reef fish larvae and other reef inhabitants (Lo-Yat et al., 2011; D'Angelo and Wiedenmann, 2014).

Previous studies have shown that our sampled reef area has a high density of fish larvae when compared to other habitats in the region (Mota et al., 2017), and it has even been suggested as a larval export source (Freitas et al., 2019). The presence of reef-building corals in our sampled area (Soares et al., 2017, 2019b; Costa et al., 2024) could increase the supply of nutrients to the water column, being probably rapidly consumed by phytoplankton, which could explain the greater

abundance of fish larvae in this area relative to the surrounding area. Indeed, laboratory experiments have shown that coral exudates increase bacterial biomass by 6 times and autotrophic biomass (cyanobacteria and flagellates) by 3–5 times (Ferrier-Pagès et al., 2000). Coral exudates can not only directly impact phytoplankton biomass, but also exert indirect effects, as the remineralization of nutrients by bacterioplankton meets the nutritional needs of phytoplankton (Hopkinson et al., 1987).

However, it is important to note that despite the potential increase in phytoplankton biomass due to the presence of reef-building corals, the abundant fish larvae (Mota et al., 2017), corals, sponges (Soares et al., 2017), zooplankton and other herbivores that inhabit reef areas can also control the increase in phytoplankton biomass by feeding on these organisms (top-down effects) (Lesser, 2006; Genin et al., 2009; Anneville et al., 2019), contributing to the balance of the reef ecosystem.

4.2. Phytoplankton assemblages

In this study, diatoms (type 1 and type 2), picocyanobacteria (*Synechococcus* and *Prochlorococcus*, the latter genus to a lesser extent), and prymnesiophytes contributed the most to the total biomass. However, the distribution of phytoplankton assemblages exhibited significant spatial heterogeneity as shown in NMDS (Fig. 5), with diatoms showing a higher relative contribution in the reef area (~50 %), accompanied by a stronger depletion of silica. This predominance of diatoms contrasts with expectations for an oligotrophic region, where picocyanobacteria typically dominate the phytoplankton assemblages (Charpy et al., 2012; Farias et al., 2022). *Synechococcus* and *Prochlorococcus* belong to the picophytoplankton fraction (<2 μm) and are important components of primary production in tropical oligotrophic oceans due to their high efficiency in assimilating nutrients at low concentrations (Agawin et al., 2000; Carneiro et al., 2022).

However, one hypothesis to explain the higher contribution of diatoms at the expense of picocyanobacteria in the reef area could be that diatoms are also being sustained by the release of organic nutrients (Cochlan et al., 2008; Loureiro et al., 2009) from sessile suspension feeders (e.g., sponges) through benthic–pelagic coupling. Notably, high fractions of diatoms and low of *Synechococcus* also were reported in the Caribbean reefs (Curaçao), with the benthic filter feeders preferring small cell fractions (Van Duyl et al., 2002), pointing out that benthic-pelagic coupling in the reef area can take place in different ways, such as nutrient enrichment and feeding selectivity.

In this sense, although the all study area is shallow and favorable to benthic-pelagic coupling, the distinct nature of the bottom in the reef area may intensify this process. Indeed, another study in the area has corroborated the spatial heterogeneity in relation to partial pressure of CO_2 (pCO_2) in the water (Cotovicz et al., 2020). In this study, coral reef waters in the SAC region act as sources of CO_2 to the atmosphere due to net calcium carbonate ($CaCO_3$) precipitation by shallow-water reefs (Cotovicz et al., 2020).

Additionally, the high degree of mixing of the water column in the entire study area is another factor that likely favors diatoms in relation to the other groups, even in the absence of reefs. This is because turbulence keeps diatoms (non-motile and heavy organisms) suspended in the euphotic zone, helping them compete for light and nutrient assimilation (Reynolds, 2006; Villamaña et al., 2019). In this way, in a shallow continental shelf, such as the sampled area, the resuspension of nutrients from the sediment into the water column is more effective (Margalef, 1978; Cullen et al., 2002; Glibert, 2016; Islabão et al., 2017; Villamaña et al., 2019), influencing phytoplankton assemblages. However, as indicated by our data, the differentiated bottom of the reef area (e.g., inside MPA) leads to more intense biogeochemical processes.

Another prevalent group in the SAC, the prymnesiophytes (Haptophytes), occur in both coastal and oceanic environments (Eikrem et al., 2017). The relative contribution of prymnesiophytes to Tchl *a* concentration in the SAC was higher (10–40 %) than those in the Abrolhos coral reef area, an environment enriched with DIN (Knoppers et al., 1999b). In this way, a higher contribution of prymnesiophytes in the oligotrophic waters of the SAC may be related to their high affinity for assimilating nitrate (Litchman et al., 2007) and phosphate (Riegman et al., 2000) at low concentrations.

On the other hand, the relative contribution of *Synechococcus*, which was higher than that of *Prochlorococcus*, was consistent with the average abundance data for these genera (*Synechococcus* = 7.93×10^6 cells L^{-1}; *Prochlorococcus* = 2.76×10^6 cells L^{-1}) obtained via flow cytometry in the SAC (Saes, 2018). Although *Synechococcus* contributed more than *Prochlorococcus* at all stations, the latter's contribution increased at the station furthest from the coast (S10), which aligns with previous global reports that show an increase in *Prochlorococcus* with distance from the coast (Jacquet et al., 2006; Carreto et al., 2008; Zhou et al., 2018). Similar behavior was found in research reports from other shallow tropical regions (Knoppers et al., 1999b; Farias et al., 2022).

Additionally, it is important to highlight that the green flagellate, dinoflagellate, and cryptophyte groups were responsible for a small contribution to Tchl *a* (<10 %) in the SAC. These data are consistent with previous research in the southwest tropical Atlantic (Knoppers et al., 1999b; Farias et al., 2022). Although dinoflagellates are adapted to oligotrophic waters and include even mixotrophic species, they prefer low-turbulence environments (Margalef, 1978), higher N:P ratios, and chemically reduced forms of nitrogen (Glibert, 2016), which was opposite to our findings in the study area.

5. Conclusions and final considerations

In conclusion, we found that despite the horizontal environmental homogeneity characterized by minimal variations in salinity and temperature, the nutrients (mainly, DSi) and relative contributions of diatoms, picocyanobacteria and prymnesiophytes to the total biomass exhibited significant heterogeneity. Notably, stations influenced by tropical reefs (with significant sponge and coral cover) (Soares et al., 2017; Carneiro et al., 2022) differed from adjacent reefless waters in composition of the phytoplanktonic assemblages, but no significant difference was found between the areas in total biomass. Despite this, it was possible to see an increase in relative contribution of diatoms in the reef area, which contributed to silica depletion.

The benthic-pelagic coupling could be relevant for the whole area given the well-mixed water column resulting from the intense hydrodynamic factors and because it is a shallow environment. However, the differentiated bottom of the reef area can lead to more intense biogeochemical processes as reflected by differentiated spatial signature of nutrients and phytoplankton composition (as detected by HPLC-CHEMTAX).

Finally, our data sheds light on phytoplankton assemblages in oligotrophic areas influenced by tropical reefs, demonstrating that, contrary to what is currently expected, other groups besides picocyanobacteria, such as diatoms, may be the group that contributes most to biomass. Additionally, we expanded our knowledge about the phytoplankton assemblages in the Equatorial Southwestern Atlantic by also demonstrating the importance of prymnesiophytes, a group that is still poorly detected in conventional microscopy analyses.

CRediT authorship contribution statement

Antonia Diana Alves Bezerra: Writing – review & editing, Writing – original draft, Validation, Supervision, Investigation, Formal analysis, Conceptualization. **Hortência de Sousa Barroso:** Writing – review & editing, Writing – original draft, Supervision, Resources, Funding acquisition, Formal analysis. **Carlos Rafael Borges Mendes:** Writing – review & editing, Writing – original draft, Formal analysis. **Luiz C. Cotovicz:** Writing – review & editing, Writing – original draft. **Tallita Cruz Lopes Tavares:** Writing – review & editing, Writing – original draft, Formal analysis. **Tatiane Martins Garcia:** Writing – review & editing, Writing – original draft. **Michael Barbosa Viana:** Writing –

review & editing, Writing – original draft. **Marcelo Oliveira Soares:** Writing – review & editing, Writing – original draft, Validation, Project administration, Investigation, Funding acquisition, Formal analysis, Data curation, Conceptualization.

Declaration of competing interest

- This manuscript has not been submitted to, nor is under review at, another journal or other publishing venue.
- The authors have no affiliation with any organization with a direct or indirect financial interest in the subject matter discussed in the manuscript
- The author(s) declare no competing (financial or non-financial) interests.

Acknowledgments

This research was supported by FUNBIO (GEF-MAR), PELD Costa Semiárida do Brasil-CSB (National Council for Scientific and Technological Development CNPq No. 442337/2020-5, 445974/2024-9, 444172/2024-6 and Cearense Foundation for the Support of Scientific and Technological Development FUNCAP N. PEL-00177-00005.01.00/21). We thank CAPES-PRINT, CAPES-PNPD, CAPES-COFECUB, CAPES-Alexander Von Humboldt Foundation, CNPq Research Productiviy Fellowship (No. 313518/2020-3), and FUNCAP (Chief Scientist Program) for their financial support. H.S. Barroso thanks the researcher fellowships of the PELD CSB (DTI-A, CNPq) and Blue University project (SET-A, CNPq; proc. No. 409682/2022-5). A.D.A. Bezerra thanks the researcher fellowships of the Blue University project (DTI-C, CNPq).

Appendix A. Supplementary data

Supplementary data to this article can be found online at https://doi.org/10.1016/j.scitotenv.2024.178253.

Data availability

Data will be made available on request.

References

Agawin, N.S.R., Duarte, C.M., Agustí, S., 2000. Nutrient and temperature control of the contribution of picoplankton to phytoplankton biomass and production. Limnol. Oceanogr. 45, 591–600. https://doi.org/10.4319/lo.2000.45.3.0591.

Aminot, A., Chaussepied, M., 1983. Manuel des analyses chimiques en Milieu Marin. Centre National pour l'Exploration des Oceans, Brest.

Anneville, O., Chang, C., Dur, G., Souissi, S., Rimet, F., Hsieh, C., 2019. The paradox of re-oligotrophication: the role of bottom–up versus top–down controls on the phytoplankton community. Oikos 128, 1666–1677. https://doi.org/10.1111/oik.06399.

Araujo, M., Noriega, C., Medeiros, C., Lefèvre, N., Ibánhez, J.S.P., Flores Montes, M., Silva, A.C.D., Santos, M.D.L., 2019. On the variability in the CO2 system and water productivity in the western tropical Atlantic off North and Northeast Brazil. J. Mar. Syst. 189, 62–77. https://doi.org/10.1016/j.jmarsys.2018.09.008.

Bakker, J.D., 2024. ANOSIM. Applied Multivariate Statistics in R.

Barroso, H.D.S., Lima, I.D.O., Bezerra, A.D.A., Garcia, T.M., Tavares, T.C.L., Alves, R.S., Souza Junior, E.F.D., Teixeira, C.E.P., Viana, M.B., Soares, M.O., 2023. Distribution of nutrients and chlorophyll across an equatorial reef region: insights on coastal gradients. Ocean Coast. Res. 71, e23002. https://doi.org/10.1590/2675-2824071.22016hdsb.

Baumgarten, M.G.Z., Rocha, J.M.B., Niencheski, L.F.H., 1996. Manual de análises em oceanografia química, 1st ed. Editora da Furg, Rio Grande.

Bell, P.R.F., Greenfield, P.F., Hawker, D., Connell, D., 1989. The impact of waste discharges on coral reef regions. Water Sci. Technol. 21, 121–130. https://doi.org/10.2166/wst.1989.0014.

Bell, P.R.F., Elmetri, I., Lapointe, B.E., 2014. Evidence of large-scale chronic eutrophication in the great barrier reef: quantification of chlorophyll a thresholds for sustaining coral reef communities. AMBIO 43, 361–376. https://doi.org/10.1007/s13280-013-0443-1.

Borcard, D., Gillet, F., Legendre, P., Borcard, D., Gillet, F., Legendre, P., 2018. Spatial analysis of ecological data. Numerical Ecology With R 299–367.

Brito, A.C., Sá, C., Mendes, C.R., Brand, T., Dias, A.M., Brotas, V., Davidson, K., 2015. Structure of late summer phytoplankton community in the Firth of Lorn (Scotland) using microscopy and HPLC-CHEMTAX. Estuar. Coast. Shelf Sci. 167, 86–101. https://doi.org/10.1016/j.ecss.2015.07.006.

Bruce, T., Meirelles, P.M., Garcia, G., Paranhos, R., Rezende, C.E., de Moura, R.L., Filho, R.-F., Coni, E.O.C., Vasconcelos, A.T., Amado Filho, G., Hatay, M., Schmieder, R., Edwards, R., Dinsdale, E., Thompson, F.L., 2012. Abrolhos bank reef health evaluated by means of water quality, microbial diversity, benthic cover, and fish biomass data. PLoS One 7, e36687. https://doi.org/10.1371/journal.pone.0036687.

Brzezinski, M.A., 1985. The Si: C: N ratio of marine diatoms: interspecific variability and the effect of some environmental variables. J. Phycol. 21, 347–357.

Carneiro, P.B. de M., Morais, J.O. de, 2016. Carbonate sediment production in the equatorial continental shelf of South America: quantifying Halimeda incrassata (Chlorophyta) contributions. J. S. Am. Earth Sci. 72, 1–6. https://doi.org/10.1016/j.jsames.2016.07.011.

Carneiro, P.B. de M., Lima, J.P. de, Bandeira, Ê.V.P., Ximenes Neto, A.R., Rocha Barreira, C. de A., Tâmega, F.T. de S., Matthews-Cascon, H., Franklin Junior, W., Morais, J.O. de, 2021. Structure, growth and CaCO3 production in a shallow rhodolith bed from a highly energetic siliciclastic-carbonate coast in the equatorial SW Atlantic Ocean. Mar. Environ. Res. 166, 105280. https://doi.org/10.1016/j.marenvres.2021.105280.

Carneiro, P.B.M., Ximenes Neto, A.R., Jucá-Queiroz, B., Teixeira, C.E.P., Feitosa, C.V., Barroso, C.X., Matthews-Cascon, H., de Morais, J.O., Freitas, J.E.P., Santander-Neto, J., de Araújo, J.T., Monteiro, L.H.U., Pinheiro, L.S., Braga, M.D.A., Cordeiro, R. T.S., Rossi, S., Bejarano, S., Salani, S., Garcia, T.M., Lotufo, T.M.C., Smith, T.B., Faria, V.V., Soares, M.O., 2022. Interconnected marine habitats form a single continental-scale reef system in South America. Sci. Rep. 12, 17359. https://doi.org/10.1038/s41598-022-21341-x.

Carreto, J.I., Montoya, N., Akselman, R., Carignan, M.O., Silva, R.I., Cucchi Colleoni, D. A., 2008. Algal pigment patterns and phytoplankton assemblages in different water masses of the Río de la Plata maritime front. Cont. Shelf Res. 28, 1589–1606. https://doi.org/10.1016/j.csr.2007.02.012.

Carvalho, A.C.O., Marins, R.V., Dias, F.J.S., Rezende, C.E., Lefèvre, N., Cavalcante, M.S., Eschrique, S.A., 2017. Air-sea CO 2 fluxes for the Brazilian northeast continental shelf in a climatic transition region. J. Mar. Syst. 173, 70–80. https://doi.org/10.1016/j.jmarsys.2017.04.009.

Charpy, L., Casareto, B.E., Langlade, M.J., Suzuki, Y., 2012. Cyanobacteria in coral reef ecosystems: a review. J. Mar. Biol. 2012, 1–9. https://doi.org/10.1155/2012/259571.

Cochlan, W.P., Herndon, J., Kudela, R.M., 2008. Inorganic and organic nitrogen uptake by the toxigenic diatom Pseudo-nitzschia australis (Bacillariophyceae). Harmful Algae 8, 111–118. https://doi.org/10.1016/j.hal.2008.08.008.

Cole, G.A., 1983. Textbook of Limnology. Waveland Press, Illinois, USA.

Costa, R.J., De Macedo Carneiro, P.B., Feitosa, C.V., De Sousa Barroso, H., Da Silva, M.V. C., Giarrizzo, T., Salani, S., Gastão, F.G.C., Garcia, T.M., Tavares, T.C.L., Smith, T.B., Soares, M.O., 2024. Depth drive shifts in the fish and benthic assemblages of the South American Reef System. Sci. Rep. 14, 29607. https://doi.org/10.1038/s41598-024-76641-1.

Cotovicz, L.C., Chielle, R., Marins, R.V., 2020. Air-sea CO2 flux in an equatorial continental shelf dominated by coral reefs (Southwestern Atlantic Ocean). Cont. Shelf Res. 204, 104175. https://doi.org/10.1016/j.csr.2020.104175.

Crosbie, N., Furnas, M., 2001. Net growth rates of picocyanobacteria and nano-microphytoplankton inhabiting shelf waters of the central (17S) and southern (20S) Great Barrier Reef. Aquat. Microb. Ecol. 24, 209–224. https://doi.org/10.3354/ame024209.

Cullen, J.J., Franks, P.J.S., Karl, D.M., Longhurst, A., 2002. Physical influences on marine ecosystem dynamics. In: Robinson, A.R., McCarthy, J.J., Rothschild, B.J. (Eds.), The Sea. Vol. 12: Biological-Physical Interactions in the Ocean. John Wiley & Sons, New York, pp. 297–335.

D'Angelo, C., Wiedenmann, J., 2014. Impacts of nutrient enrichment on coral reefs: new perspectives and implications for coastal management and reef survival. Curr. Opin. Environ. Sustain. 7, 82–93. https://doi.org/10.1016/j.cosust.2013.11.029.

Dias, F.J.S., Castro, B.M., Lacerda, L.D., 2013. Continental shelf water masses off the Jaguaribe River (4S), northeastern Brazil. Cont. Shelf Res. 66, 123–135. https://doi.org/10.1016/j.csr.2013.06.005.

Domingues, R.B., Nogueira, P., Barbosa, A.B., 2023. Co-limitation of phytoplankton by N and P in a shallow coastal lagoon (Ria Formosa): implications for eutrophication evaluation. Estuar. Coasts 46, 1557–1572.

Edler, L., Elbrächter, M., 2010. The Utermöhl method for quantitative phytoplankton analysis. In: Karlson, B., Cusack, C., Bresnan, E. (Eds.), Microscopic and Molecular Methods for Quantitative Phytoplankton Analysis. Intergovernmental Oceanographic Commission of Unesco, Paris, pp. 1–114. https://doi.org/10.25607/OBP-1371.

Eikrem, W., Medlin, L.K., Henderiks, J., Rokitta, S., Rost, B., Probert, I., Throndsen, J., Edvardsen, B., 2017. Haptophyta. In: Archibald, J.M., Simpson, A.G.B., Slamovits, C. H., Margulis, L., Melkonian, M., Chapman, D.J., Corliss, J.O. (Eds.), Handbook of the Protists. Springer International Publishing, Cham, pp. 1–61. https://doi.org/10.1007/978-3-319-32669-6_38-2.

Elser, J.J., Bracken, M.E.S., Cleland, E.E, Gruner, D.S., Harpole, W.S., Hillebrand, H., Ngai, J. T., Seabloom, E.W., Shurin, J.B., Smith J.E., 2007. Global analysis of nitrogen and phosphorus limitation of primary producers in freshwater, marine and terrestrial ecosystems. Ecology Ecology Letters, 10: 1135. doi:https://doi.org/10.1111/j.1461-0248.2007.01113.x.

Farias, G.B., Molinero, J.-C., Carré, C., Bertrand, A., Bec, B., Melo, P.A.M. de C., 2022. Uncoupled changes in phytoplankton biomass and size structure in the western

tropical Atlantic. J. Mar. Syst. 227, 103696. doi:https://doi.org/10.1016/j.jmarsys.2021.103696.
Ferrier-Pagès, C., Leclercq, N., Jaubert, J., Pelegrí, S., 2000. Enhancement of pico- and nanoplankton growth by coral exudates. Aquat. Microb. Ecol. 21, 203–209. https://doi.org/10.3354/ame021203.
Field, C.B., Behrenfeld, M.J., Randerson, J.T., Falkowski, P., 1998. Primary production of the biosphere: integrating terrestrial and oceanic components. Science 281, 237–240. https://doi.org/10.1126/science.281.5374.237.
Franco, A. de O. da R., Soares, M. de O., Moreira, M.O.P., 2018. Diatom accumulations on a tropical meso-tidal beach: environmental drivers on phytoplankton biomass. Estuar. Coast. Shelf Sci. 207, 414–421. https://doi.org/10.1016/j.ecss.2017.07.020.
Freitas, J.E.P.D., Araújo, M.E.D., Lotufo, T.M.D.C., 2019. Composition and structure of the ichthyofauna in a marine protected area in the western equatorial Atlantic: a baseline to support conservation management. Reg. Stud. Mar. Sci. 25, 100488. https://doi.org/10.1016/j.rsma.2018.100488.
Furnas, M.J., Mitchell, A.W., Gilmartin, M., Revelante, N., 1990. Phytoplankton biomass and primary production in semi-enclosed reef lagoons of the central Great Barrier Reef, Australia. Coral Reefs 9, 1–10. https://doi.org/10.1007/BF00686716.
Genin, A., Monismith, S.G., Reidenbach, M.A., Yahel, G., Koseff, J.R., 2009. Intense benthic grazing of phytoplankton in a coral reef. Limnol. Oceanogr. 54, 938–951. https://doi.org/10.4319/lo.2009.54.3.0938.
Glibert, P.M., 2016. Margalef revisited: a new phytoplankton mandala incorporating twelve dimensions, including nutritional physiology. Harmful Algae 55, 25–30. https://doi.org/10.1016/j.hal.2016.01.008.
Guo, J., Yu, K., Wang, Y., Zhang, R., Huang, X., Qin, Z., 2019. Potential impacts of anthropogenic nutrient enrichment on coral reefs in the South China Sea: evidence from nutrient and chlorophyll *a* levels in seawater. Environ Sci Process Impacts 21, 1745–1753. https://doi.org/10.1039/C9EM00331B.
Guzmán, H., Cortés, J., Glynn, P., Richmond, R., 1990. Coral mortality associated with dino-flagellate blooms in the eastern Pacific (Costa Rica and Panama). Mar. Ecol. Prog. Ser. 60, 299–303. https://doi.org/10.3354/meps060299.
Hammer, Ø., Harper, D.A.T., Ryan, P.D., 2001. PAST: paleontological statistics software package for education and data analysis. Paleontol. Electron. 4, 1–9.
Higgins, H.W., Wright, S.W., Schlüter, L., 2011. Quantitative interpretation of chemotaxonomic pigment data. In: Roy, S., Llewellyn, C., Egeland, E.S., Johnsen, G. (Eds.), Phytoplankton Pigments: Characterization, Chemotaxonomy and Applications in Oceanography. Cambridge University Press, United Kingdom, pp. 257–313.
Hillebrand, H., Acevedo-Trejos, E., Moorthi, S.D., Ryabov, A., Striebel, M., Thomas, P.K., Schneider, M., 2022. Cell size as driver and sentinel of phytoplankton community structure and functioning. Funct. Ecol. 36, 276–293. https://doi.org/10.1111/1365-2435.13986.
Hoadley, K.D., Hamilton, M., Poirier, C.L., Choi, C.J., Yung, C.-M., Worden, A.Z., 2021. Selective uptake of pelagic microbial community members by Caribbean reef corals. Appl. Environ. Microbiol. 87, e03175-20. https://doi.org/10.1128/AEM.03175-20.
Hopkinson, C.S., Sherr, B.F., Ducklow, H.W., 1987. Microbial regeneration of ammonium in the water column of Davies Reef. Australia. Mar. Ecol. Prog. Ser. 41, 147–153. https://doi.org/10.3354/meps041147.
Houlbrèque, F., Delesalle, B., Blanchot, J., Montel, Y., Ferrier-Pagès, C., 2006. Picoplankton removal by the coral reef community of La PrÉvoyante, Mayotte Island. Aquat. Microb. Ecol. 44, 59–70. https://doi.org/10.3354/ame044059.
Islabão, C.A., Mendes, C.R.B., Detoni, A.M.S., Odebrecht, C., 2017. Phytoplankton community structure in relation to hydrographic features along a coast-to-offshore transect on the SW Atlantic Continental Shelf. Cont. Shelf Res. 151, 30–39. https://doi.org/10.1016/j.csr.2017.10.003.
Jacquet, S., Delesalle, B., Torréton, J.-P., Blanchot, J., 2006. Response of phytoplankton communities to increased anthropogenic influences(southwestern lagoon, New Caledonia). Mar. Ecol. Prog. Ser. 320, 65–78. https://doi.org/10.3354/meps320065.
Jales, M.C., Feitosa, F.A.D.N., Koening, M.L., Montes, M.D.J.F., Araújo Filho, M.C.D., Silva, R.A.D., 2015. Phytoplankton biomass dynamics and environmental variables around the Rocas Atoll Biological Reserve, South Atlantic. Braz. J. Oceanogr. 63, 443–454. https://doi.org/10.1590/S1679-87592015093906304.
Jales, M.C., Feitosa, F.A.N., Koening, M.L., Montes, M.D.J.F., Pedrosa, V.B., 2021. Influence of abiotic factors on phytoplankton diversity and distribution in an atoll environment. Acta Bot. Bras. 35, 503–516. https://doi.org/10.1590/0102-33062020abb0269.
Jeffrey, S.W., Wright, S.W., Zapata, M., 2011. Microalgal classes and their signature pigments. In: Roy, S., Llewellyn, C.A., Egeland, E.S., Johnsen, G. (Eds.), Phytoplankton Pigments: Characterization, Chemotaxonomy and Applications in Oceanography. Cambridge University Press, United Kingdom, pp. 3–77.
Justić, D., Rabalais, N.N., Turner, R.E., Dortch, Q., 1995. Changes in nutrient structure of river-dominated coastal waters: stoichiometric nutrient balance and its consequences. Estuar. Coast. Shelf Sci. 40, 339–356. https://doi.org/10.1016/S0272-7714(05)80014-9.
Ke, Z., Liu, H., Wang, J., Liu, J., Tan, Y., 2016. Abnormally high phytoplankton biomass near the lagoon mouth in the Huangyan Atoll, South China Sea. Mar. Pollut. Bull. 112, 123–133. https://doi.org/10.1016/j.marpolbul.2016.08.028.
Keighan, R., Van Woesik, R., Yalon, A., Nam, J., Houk, P., 2023. Moderate chlorophyll-a environments reduce coral bleaching during thermal stress in Yap. Micronesia. Sci. Rep. 13, 9338. https://doi.org/10.1038/s41598-023-36355-2.
Klein, V.L.M., 1977. Sobre a composição e abundância relativa do plâncton, na plataforma continental do Estado do Ceará. Arq. Ciênc. Mar 17, 21–27.
Knoppers, B., Ekau, W., Figueiredo, A.G., 1999a. The coast and shelf of east and northeast Brazil and material transport. Geo-Mar. Lett. 19, 171–178. https://doi.org/10.1007/s003670050106.
Knoppers, B., Meyerhöfer, M., Marone, E., Dutz, J., Lopes, R., Leipe, T., De Camargo, R., 1999b. Compartments of the pelagic system and material exchange at the Abrolhos bank coral reefs. Brazil. Arch. Fish. Mar. Res. 47, 285–306.
Lesser, M.P., 2006. Benthic–pelagic coupling on coral reefs: feeding and growth of Caribbean sponges. J. Exp. Mar. Biol. Ecol. 328, 277–288. https://doi.org/10.1016/j.jembe.2005.07.010.
Litchman, E., Klausmeier, C.A., Schofield, O.M., Falkowski, P.G., 2007. The role of functional traits and trade-offs in structuring phytoplankton communities: scaling from cellular to ecosystem level. Ecol. Lett. 10, 1170–1181. https://doi.org/10.1111/j.1461-0248.2007.01117.x.
Loureiro, S., Jauzein, C., Garces, E., Collos, Y., Camp, J., Vaque, D., 2009. The significance of organic nutrients in the nutrition of Pseudo-nitzschia delicatissima (Bacillariophyceae). J. Plankton Res. 31, 399–410. https://doi.org/10.1093/plankt/fbn122.
Lo-Yat, A., Simpson, S.D., Meekan, M., Lecchini, D., Martinez, E., Galzin, R., 2011. Extreme climatic events reduce ocean productivity and larval supply in a tropical reef ecosystem: ENSO AND LARVAL RECRUITMENT. Glob. Chang. Biol. 17, 1695–1702. https://doi.org/10.1111/j.1365-2486.2010.02355.x.
Mackey, M.D., Mackey, D.J., Higgins, H.W., Wright, S.W., 1996. CHEMTAX-a program for estimating class abundances from chemical markers: application to HPLC measurements of phytoplankton. Mar. Ecol. Prog. Ser. 144, 265–283. https://doi.org/10.3354/meps144265.
Margalef, R., 1978. Life-forms of phytoplankton as survival alternatives in an unstable environment. Oceanol. Acta 1, 493–509.
Mendes, C.R., Cartaxana, P., Brotas, V., 2007. HPLC determination of phytoplankton and microphytobenthos pigments: comparing resolution and sensitivity of a C18 and a C8 method. Limnol. Oceanogr. Methods 5, 363–370. https://doi.org/10.4319/lom.2007.5.363.
Mendes, C.R.B., Odebrecht, C., Tavano, V.M., Abreu, P.C., 2017. Pigment-based chemotaxonomy of phytoplankton in the Patos Lagoon estuary (Brazil) and adjacent coast. Mar. Biol. Res. 13, 22–35. https://doi.org/10.1080/17451000.2016.1189082.
Menezes, M., Junger, P.C., Kavagutti, V.S., Wanderley, B., Cabral, A.D.S., Paranhos, R., Unrein, F., Amado, A.M., Sarmento, H., 2023. Temporal patterns of picoplankton abundance and metabolism on the western coast of the equatorial Atlantic Ocean. Ocean Coast. Res. 71, e23019. https://doi.org/10.1590/2675-2824071.22048mm.
Moreira Filho, H., Eskinazi-Leça, E., Valente-Moreira, I.M., Cunha, J.A., 1999. Avaliação taxonômica e ecológica das diatomáceas (Chrysophyta - Bacillariophyceae) marinhas e estuarinas nos estados de Pernambuco, Paraíba, Rio Grande do Norte, Ceará, Piauí, Maranhão, Pará e Amapá. Brasil. Trop. Oceanogr. 27. https://doi.org/10.5914/tropocean.v27i1.2773.
Mota, E.M.T., Garcia, T.M., Freitas, J.E.P., Soares, M.O., 2017. Composition and cross-shelf distribution of ichthyoplankton in the Tropical Southwestern Atlantic. Reg. Stud. Mar. Sci. 14, 27–33. https://doi.org/10.1016/j.rsma.2017.05.001.
Oksanen, J., Simpson, G.L., Blanchet, F.G., Kindt, R., Legendre, P., Minchin, P.R., O'Hara, R.B., Solymos, P., Stevens, M.H.H., Szoecs, E., et al., 2024. Vegan: community ecology package. Available online: https://cran.r-project.org/web/packages/vegan/index.htm.
Passavante, J.Z.D.O., Koening, M.L., Eskinazi-Leça, E., 1982. Dinoflagelados da plataforma continental do Ceará. Trop. Oceanogr. 17. https://doi.org/10.5914/tropocean.v17i1.2604.
Pauly, D., Christensen, V., 1995. Primary production required to sustain global fisheries. Nature 374, 255–257. https://doi.org/10.1038/374255a0.
Pauly, D., Christensen, V., Guénette, S., Pitcher, T.J., Sumaila, U.R., Walters, C.J., Watson, R., Zeller, D., 2002. Towards sustainability in world fisheries. Nature 418, 689–695. https://doi.org/10.1038/nature01017.
Pomati, F., Shurin, J.B., Andersen, K.H., Tellenbach, C., Barton, A.D., 2020. Interacting temperature, nutrients and zooplankton grazing control phytoplankton size-abundance relationships in eight Swiss lakes. Front. Microbiol. 10, 3155. https://doi.org/10.3389/fmicb.2019.03155.
Redfield, A.C., Ketchum, B.H., Richards, F.A., 1963. The influence of organisms on the composition of the sea water. In: The Sea. Interscience Publishers, New York.
Ren, L., Rabalais, N.N., Turner, R.E., Morrison, W., Mendenhall, W., 2009. Nutrient limitation on phytoplankton growth in the Upper Barataria Basin, Louisiana: microcosm bioassays, Louisiana: Microcosm Bioassays. Estuar. Coasts 32, 958–974. https://doi.org/10.1007/s12237-009-9174-8.
Reynolds, C.S., 2006. The Ecology of Phytoplankton. Cambridge University Press, New York.
Ribes, M., Coma, R., Atkinson, M.J., Kinzie, R.A., 2005. Sponges and ascidians control removal of particulate organic nitrogen from coral reef water. Limnol. Oceanogr. 50, 1480–1489. https://doi.org/10.4319/lo.2005.50.5.1480.
Riegman, R., Stolte, W., Noordeloos, A.A.M., Slezak, D., 2000. Nutrient uptake and alkaline phosphatase (EC 3:1:3:1) activity of Emiliania Huxleyi (Prymnesiophyceae) during growth under N and P limitation in continuous cultures. J. Phycol. 36, 87–96. https://doi.org/10.1046/j.1529-8817.2000.99023.x.
Roelfsema, C., Phinn, S., Jupiter, S., Comley, J., Albert, S., 2013. Mapping coral reefs at reef to reef-system scales, 10s–1000s km^2, using object-based image analysis. Int. J. Remote Sens. 34, 6367–6388. doi:https://doi.org/10.1080/01431161.2013.800660.
Rossi, S., Gili, J.-M., 2009. Near bottom phytoplankton and seston: importance in the pelagic-benthic coupling processes. Mar. Phytoplankton 45–85.
Saes, R.V. da S.T., 2018. Diversidade e estoque de carbono em cianobactérias na costa e nos arquipélagos da porção oeste do giro Equatorial Atlântico (Tese (Doutorado em Ciências Marinhas Tropicais)). Universidade Federal do Ceará, Ceará.
Schlitzer, R., 2016. Ocean Data View.
Schlüter, L., Henriksen, P., Nielsen, T.G., Jakobsen, H.H., 2011. Phytoplankton composition and biomass across the southern Indian Ocean. Deep Sea Res. Part Oceanogr. Res. Pap. 58, 546–556. https://doi.org/10.1016/j.dsr.2011.02.007.

Simpson, J., Sharples, J., 2012. Introduction to the Physical and Biological Oceanography of Shelf Seas. Cambridge University Press, Cambridge.

Soares, M. de O., Paiva, C.C. de, Freitas, J.E.P. de, Lotufo, T.M. da C., 2011. Gestão de unidades de conservação marinhas: o caso do Parque Estadual Marinho da Pedra da Risca do Meio, NE – Brasil. Rev. Gest. Costeira Integrada 11, 257–268. https://doi.org/10.5894/rgci261.

Soares, M.O., Rossi, S., Martins, F.A.S., Carneiro, P.B.D.M., 2017. The forgotten reefs: benthic assemblage coverage on a sandstone reef (Tropical South-western Atlantic). J. Mar. Biol. Assoc. U. K. 97, 1585–1592. https://doi.org/10.1017/S0025315416000965.

Soares, M.O., Teixeira, C.E.P., Ferreira, S.M.C., Gurgel, A.L.A.R., Paiva, B.P., Menezes, M. O.B., Davis, M., Tavares, T.C.L., 2019a. Thermal stress and tropical reefs: mass coral bleaching in a stable temperature environment? Mar. Biodivers. 49, 2921–2929. https://doi.org/10.1007/s12526-019-00994-4.

Soares, M.O., Tavares, T.C.L., Carneiro, P.B.D.M., 2019b. Mesophotic ecosystems: distribution, impacts and conservation in the South Atlantic. Divers. Distrib. 25, 255–268. https://doi.org/10.1111/ddi.12846.

Soares, M.O., Campos, C.C., Carneiro, P.B.M., Barroso, H.S., Marins, R.V., Teixeira, C.E. P., Menezes, M.O.B., Pinheiro, L.S., Viana, M.B., Feitosa, C.V., Sánchez-Botero, J.I., Bezerra, L.E.A., Rocha-Barreira, C.A., Matthews-Cascon, H., Matos, F.O., Gorayeb, A., Cavalcante, M.S., Moro, M.F., Rossi, S., Belmonte, G., Melo, V.M.M., Rosado, A.S., Ramires, G., Tavares, T.C.L., Garcia, T.M., 2021. Challenges and perspectives for the Brazilian semi-arid coast under global environmental changes. Perspect. Ecol. Conserv. 19, 267–278. https://doi.org/10.1016/j.pecon.2021.06.001.

Sospedra, J., Niencheski, L.F.H., Falco, S., Andrade, C.F.F., Attisano, K.K., Rodilla, M., 2018. Identifying the main sources of silicate in coastal waters of the Southern Gulf of Valencia (Western Mediterranean Sea). Oceanologia 60, 52–64. https://doi.org/10.1016/j.oceano.2017.07.004.

Souto, L. de S., Souto, E. de S., 2020. Análise de dados ecológicos: um guia simplificado de análises estatísticas para estudantes e profissionais da área ambiental, 1st ed. Ed. do autor, Brasília.

Stock, C.A., John, J.G., Rykaczewski, R.R., Asch, R.G., Cheung, W.W.L., Dunne, J.P., Friedland, K.D., Lam, V.W.Y., Sarmiento, J.L., Watson, R.A., 2017. Reconciling fisheries catch and ocean productivity. Proc. Natl. Acad. Sci. 114. https://doi.org/10.1073/pnas.1610238114.

Strickland, J.D.H., Parsons, T.R., 1972. A Practical Handbook of Seawater Analysis. Bulletin Fisheries Research Board of Canada, Fisheries Research Board of Canada, Ottawa, Canada.

Tada, K., Sakay, K., Nakano, Y., Takemura, A., Montani, S., 2003. Size-fractionated phytoplankton biomass in coral reef waters off Sesoko Island, Okinawa. Japan. J. Plankton Res. 25, 991–997. https://doi.org/10.1093/plankt/25.8.991.

Teixeira, C.E.P., Machado, G.T., 2013. On the temporal variability of the sea surface temperature on the tropical southwest Atlantic Continental Shelf. J. Coast. Res. 165, 2071–2076. https://doi.org/10.2112/SI65-350.1.

Tréguer, P.J., De La Rocha, C.L., 2013. The world ocean silica cycle. Annu. Rev. Mar. Sci. 5, 477–501. https://doi.org/10.1146/annurev-marine-121211-172346.

Van Duyl, F.C., Gast, G.J., Steinhoff, W., Kloff, S., Veldhuis, M.J.W., Bak, R.P.M., 2002. Factors influencing the short-term variation in phytoplankton composition and biomass in coral reef waters. Coral Reefs 21, 293–306. https://doi.org/10.1007/s00338-002-0248-3.

Villamaña, M., Marañón, E., Cermeño, P., Estrada, M., Fernández-Castro, B., Figueiras, F. G., Latasa, M., Otero-Ferrer, J.L., Reguera, B., Mouriño-Carballido, B., 2019. The role of mixing in controlling resource availability and phytoplankton community composition. Prog. Oceanogr. 178, 102181. https://doi.org/10.1016/j.pocean.2019.102181.

Vital, H., Stattegger, K., Amaro, V.E., Schwarzer, K., Frazão, E.P., Tabosa, W.F., Silveira, I.M., 2008. A modern high-energy siliciclastic-carbonate platform: continental shelf adjacent to northern Rio Grande do Norte state, northeastern Brazil. In: Hampson, G.J., Steel, R.J., Burgess, P.M., Dalrymple, R.W. (Eds.), Recent Advances in Models of Siliciclastic Shallow-marine Stratigraphy. SEPM Society for Sedimentary Geology, pp. 175–188. https://doi.org/10.2110/pec.08.90.0177.

Vollbrecht, C., Moehlenkamp, P., Gove, J.M., Neuheimer, A.B., McManus, M.A., 2021. Long-term presence of the island mass effect at Rangiroa Atoll. French Polynesia. Front. Mar. Sci. 7, 595294. https://doi.org/10.3389/fmars.2020.595294.

Waterbury, J.B., Watson, S.W., Guillard, R.R.L., Brand, L.E., 1979. Widespread occurrence of a unicellular, marine, planktonic, cyanobacterium. Nature 277, 293–294. https://doi.org/10.1038/277293a0.

Wickham, Hadley, 2016. Ggplot2: Elegrant Graphics for Data Analysis. Springer.

Wright, S.W., Jeffrey, S.W., 2006. Pigment markers for phytoplankton production. In: Volkman, J.K. (Ed.), Marine Organic Matter: Biomarkers, Isotopes and DNA, The Handbook of Environmental Chemistry. Springer-Verlag, Berlin/Heidelberg, pp. 71–104. https://doi.org/10.1007/698_2_003.

Wright, S.W., Ishikawa, A., Marchant, H.J., Davidson, A.T., Van Den Enden, R.L., Nash, G.V., 2009. Composition and significance of picophytoplankton in Antarctic waters. Polar Biol. 32, 797–808. https://doi.org/10.1007/s00300-009-0582-9.

Xia, Y., 2020. Chapter eleven - correlation and association analyses in microbiome study integrating multiomics in health and disease. In: Sun, J. (Ed.), The Microbiome in Health and Disease, Progress in Molecular Biology and Translational Science. Academic Press, pp. 309–491. https://doi.org/10.1016/bs.pmbts.2020.04.003.

Zapata, M., Rodríguez, F., Garrido, J., 2000. Separation of chlorophylls and carotenoids from marine phytoplankton:a new HPLC method using a reversed phase C8 column and pyridine-containing mobile phases. Mar. Ecol. Prog. Ser. 195, 29–45. https://doi.org/10.3354/meps195029.

Zapata, M., Rodríguez, F., Fraga, S., Barra, L., Ruggiero, M.V., 2011. Chlorophyll *c* pigment patterns in 18 species (51 strains) of the genus Pseudo-nitzschia (Bacillariophyceae). J. Phycol. 47, 1274–1280. https://doi.org/10.1111/j.1529-8817.2011.01055.x.

Zhou, J., Song, X., Zhang, C.-Y., Chen, G.-F., Lao, Y.-M., Jin, H., Cai, Z.-H., 2018. Distribution patterns of microbial community structure along a 7000-mile latitudinal transect from the Mediterranean Sea across the Atlantic Ocean to the Brazilian Coastal Sea. Microb. Ecol. 76, 592–609. https://doi.org/10.1007/s00248-018-1150-z.